Virus Research 273 (2019) 197750

Contents lists available at ScienceDirect

Virus Research

journal homepage: www.elsevier.com/locate/virusres

In silico epitope prediction and immunogenic analysis for penton base epitope-focused vaccine against hydropericardium syndrome in chicken

Faiza Aziz[a,b,1], Soban Tufail[a,b,1], Majid Ali Shah[a,b], Muhammad Salahuddin Shah[c], Mudasser Habib[c], Osman Mirza[d], Mazhar Iqbal[a,b], Moazur Rahman[a,b,*]

[a] Drug Discovery and Structural Biology group, Health Biotechnology Division, National Institute for Biotechnology and Genetic Engineering (NIBGE), P.O. Box 577, Jhang Road, Faisalabad, Pakistan
[b] Pakistan Institute of Engineering and Applied Sciences, P.O. Nilore, Islamabad, Pakistan
[c] Vaccine Development Group, Animal Sciences Division, NIAB, Faisalabad, Pakistan
[d] Department of Drug Design and Pharmacology, University of Copenhagen, Universitetsparken 2, DK-2100 Copenhagen, Denmark

ARTICLE INFO

Keywords:
Computational immunology
Recombinant vaccine
Epitope-driven vaccine
Fowl adenovirus 4
Hydropericardium syndrome
Penton base protein

ABSTRACT

Certain strains of fowl adenovirus serotype 4 (FAdV-4) of the family *Adenoviridae* are recognized to be the causative agents of Hydropericardium Syndrome (HPS) in broiler chicken. Despite the significantly spiking mortality in broilers due to HPS, not much effort has been made to design an effective vaccine against FAdV-4. The combination of immuno- and bioinformatics tools for immunogenic epitope prediction is the most recent concept of vaccine design. It reduces the time and effort required for hunting a potent vaccine candidate and is economical. Previously, we have reported the penton base protein of FAdV-4 to be a candidate for subunit vaccine against HPS. In the present study, we have computationally pre-screened promising B- and T-cell epitopes of the penton base. Multiple methods were employed for linear B-cell epitope identification; BepiPred and five other methods based on physicochemical properties of the amino acids. The penton base was homology modeled by means of Modeller 9.17 and after refinement of the model (by GalaxyRefine web server) ElliPro web tool was used to predict the discontinuous epitopes. NetMHCcons 1.1 and NetMHCIIpan 3.1 servers were used for the likelihood of peptide binding to Major Histocompatibility Complex (MHC) class I & II molecules respectively for T-cell epitope forecast. As a result, we identified the peptide stretch of 1–225 as the most promiscuous B- and T-cell epitope region in penton base Full Length (FL) protein sequence. *Escherichia coli* based expression vectors were generated containing cloned peptide stretch 1–225 (penton base$^{1-225}$) and penton base FL gene sequence. The recombinant penton base$^{1-225}$ and penton base FL proteins were expressed and purified using *Escherichia coli*-based expression system. Purification yield of penton base$^{1-225}$ was 3-fold higher compared to penton base FL. These proteins were injected in chickens to determine their competence in protection against HPS. The results showed equal protection level of the two proteins and the commercial inactivated vaccine against FAdV-4 infection. The results suggest the peptide stretch 1–225 of penton base as a valuable candidate for developing an epitope-driven vaccine to combat HPS.

1. Introduction

Fowl adenovirus serotype 4 (FAdV-4) is a non-enveloped, icosahedral particle belonging to the species *Fowl Aviadenovirus C*, genus *Aviadenovirus* of family *Adenoviridae*. The virion ranges from 70 to 90 nm in diameter and is one of the twelve serotypes of the fowl adenovirus (Hess, 2000; Mansoor et al., 2009). The Hydropericardium Syndrome (HPS), caused by FAdV-4, is a highly infectious disease of three to five weeks old broiler chicken. It is characterized by the accumulation of fluid in the pericardial sac-giving a flabby appearance to the heart, and hepatitis (McFerran and Smyth, 2000). Furthermore, it has a mortality rate of 80%, resulting considerable economic loss (Asthana et al., 2013). HPS was first reported in 1987 in Angara Goth in Karachi, Pakistan, that is why it is also known as the 'Angara Disease' (Asthana et al., 2013). Until now it has spread across a wide geographic scale including countries like Iraq (Abdulaziz and Alattar, 1991),

* Corresponding author at: Drug Discovery and Structural Biology group, Health Biotechnology Division, National Institute for Biotechnology and Genetic Engineering (NIBGE), P.O. Box 577, Jhang Road, Faisalabad, Pakistan.
E-mail addresses: moazur.rahman@fulbrightmail.org, moaz@nibge.org (M. Rahman).
[1] These authors contributed equally to this work.

https://doi.org/10.1016/j.virusres.2019.197750
Received 8 April 2019; Received in revised form 20 July 2019; Accepted 6 September 2019
Available online 08 September 2019
0168-1702/

Slovakia (Jantosovic et al., 1991), Mexico, Peru, Chile (Voss et al., 1996), South and Central America (Shafique et al., 1993; Shane, 1996), Russia (Borisov et al., 1997) and Korea (Kim et al., 2008).

The genome of FAdV-4 is non-segmented, linear double-stranded DNA of 45 kb size. It encodes a number of non-structural proteins and three major structural proteins; hexon, fiber and penton base. The penton base protein holds a morphologically prominent position at the vertex capsomeres of the capsid shell and consists of a pentamer of penton base together with two molecules of fiber (long and short). This protein is known to be involved in the secondary attachment of virus to the host cell; initial attachment is by means of the fiber protein of FAdV-4 via N-terminal tail, and also contributes in endocytosis (Shah et al., 2017a). As the virus enters the host cell, it encounters acidification in the endosome and consequently sheds the penton base (Asthana et al., 2013; Smith et al., 2010).

Presently, several vaccines are being used for the prevention of HPS, comprised of formalininactivated whole virus vaccine, prepared from FAdV-4 infected liver organ. These conventional vaccines don't always serve the purpose of protection because of insufficient quantity of virus titer, improper inactivation of virulent strain (chances of virus reversion), less efficacy, poor hygiene during preparation etc. (Shah et al., 2017b). An alternative to resolve these limitations is the use of subunit vaccines, which are particularly prepared from parts of the surface capsid proteins instead of the whole virus through recombinant DNA technology (Heldens et al., 2008; Lei et al., 2015; Pitcovskia et al., 2003). For development of subunit vaccine against HPS, a study was performed to evaluate the immunogenicity of recombinant penton base protein expressed in *Escherichia coli* in chicken. The results showed that the recombinant protein conferred higher protection (90%) against experimental FAdV-4 challenge as compared to commercial formalin-inactivated vaccine (60%) (Shah et al., 2012). Along the same lines, penton base full length (FL) protein (GenBank accession number: HE653773.1) was expressed in *E. coli* in our group as vaccine candidate. However, very small amount of penton base FL was expressed in soluble form and purification yield was quite low, as experienced previously, which impeded its application as cost-effective vaccine (Shah et al., 2012). It is generally considered that small proteins, having lower molecular weights, can be expressed in larger quantities in their native conformation as compared to those having higher molecular weight, in *E. coli* expression system (Dyson et al., 2004). Therefore, in-silico identification of antigenic portions of the penton base FL will be of great interest. It will assist in finding potent vaccine candidates that can be produced in large amounts by recombinant means, subsequently, warranting economic feasibility.

In birds, like other animals, the antigen-specific components of the antibody- and cell-mediated immune response are the B and T lymphocytes respectively. Both of these express antigen-specific receptors on their surface with a known repertoire of about 10^9 antigen-specificities for each (Erf, 1997). To date, there has been no in silico study of the B- and T-cell epitopes of the penton base (528 amino acids long; GenBank Acc. No. HE653773.1) of FAdV-4. So in this work, the discrimination of B- and T-cell epitopes from non-epitopes of the penton base of FAdV-4 was carried out by computational tools. Due to the non-availability of 3D structure of the penton base of FAdV-4, a homology model for the protein structure was also generated. This homology model was then refined and the quality of the final model was evaluated by different software tools. After establishing that the homology model is a good model, it was used to predict the discontinuous epitopes on the basis of different characteristics of the penton base 3D structure. The effectiveness of the predicted epitope region (penton base$^{1-225}$) as vaccine candidate was evaluated in chickens after its expression and purification using *E. coli* expression system.

2. Materials & methods

2.1. Retrieval of the penton base sequence

The sequence of the previously reported Pakistani isolate of penton base of FAdV-4 (Acc. No.: HE653773.1) was retrieved from the GenBank database of National Center for Biotechnology Information (https://www.ncbi.nlm.nih.gov/genbank) (Shah et al., 2012).

2.2. B-cell epitopes prediction

2.2.1. Linear or continuous epitope prediction

For the linear B-cell epitope prediction, an improved method, BepiPred (Jespersen et al., 2017)-combining the hidden Markov model with one of the best propensity scale methods, was used. It has already been shown in an earlier study that B cell epitope prediction performance can be increased by combining several methods (Yang and Yu, 2009). So other physicochemical properties of amino acids such as antigenicity (Kolaskar and Tongaonkar) (Kolaskar and Tongaonkar, 1990), surface accessibility (Emini et al.), flexibility (Karplus & Schulz) (Emini et al., 1985; Karplus and Schulz, 1985), hydrophilicity (Parker et al.) (Parker et al.) and beta-turns (Chou and Fasman) (Chou and Fasman, 1978) were also determined by the tools available at the platform of Immune Epitope Database (IEDB) Analysis Resource (http://tools.iedb.org/bcell).

The retrieved protein sequence, in FASTA format, was fed to the online tools integrated at the afore-mentioned resource. The protein sequence scanning window length for all methods was adjusted to seven residues. The thresholds were set to be 0.44 for BepiPred method and unity for other methods (Amat-ur-Rasool et al., 2015).

The final unanimous epitope results were obtained by combining the results of the six methods together making use of a previously published consensus method (Yang and Yu, 2009). This consensus method has also been used recently by Yang, et al. for the in silico B-cell epitope prediction of Per a 9 allergens of the American cockroach (Yang et al., 2016). Each of the result from the six tools was given an equal weightage of 16.67% and the consensus result was 0% epitope only if all the results were non-epitope. Likewise, if the predicted results had two, one or zero non-epitope(s), the consensus result was 66.7%, 83.3% or 100% respectively. Ultimately, only those regions with consensus epitope result spanning from 66.7 to 100% were recognized as the potent linear epitopes.

2.2.2. Structure-based epitope prediction

The penton base of FAdV-4 is not structurally characterized, therefore, the penton base protein sequence retrieved from GenBank (Acc. No.: HE653773.1) was fed to NCBI (National Center for Biotechnology Information) BLAST (Basic Local Alignment Search Tool) (https://blast.ncbi.nlm.nih.gov/Blast.cgi?PAGE=Proteins) to search for structural templates from Protein Data Bank (Altschul et al., 1990). Modeller 9.17 was then used to build the corresponding comparative models for the protein (Webb and Sali, 2014).

Once the homology model was derived, loop refinement was carried out by Modeller 9.17 followed by refinement with GalaxyRefine server (Heo et al., 2013). The comparative model was then validated by submitting the predicted structure to different servers like PROCHECK (Laskowski et al., 1993), PROQ (Cristobal et al., 2001), VERIFY3D (Bowie et al., 1991; Lüthy et al., 1992), ProSA-web (Wiederstein and Sippl, 2007) and ERRAT (Colovos and Yeates, 1993). The overall quality assessment of the predicted homology model was then carried out by ProTSAV which is an ensemble protein validation server (Singh et al., 2016). Furthermore, the validation modules of ProtSav were also computed for the template crystal structure (4AQQ). Results from ProTSAV for both the structures were then compared.

For the discontinuous epitope prediction, the refined model of the penton base in PDB format was served to a web tool named ElliPro

(Ponomarenko et al., 2008). The threshold values for minimum Protrusion Index (PI) and maximum distance (for grouping discontinuous epitopes) were selected as 70% and 6 Å respectively (Amat-ur-Rasool et al., 2015).

2.3. T-cell epitope prediction

The peptides binding with MHC class I and II molecules were identified to predict T cell immunogenicity as described (Andreatta et al., 2015; Karosiene et al., 2012).

2.3.1. Best human substitute alleles

There was no data regarding chicken MHC alleles available in the immunoinformatics tools used for MHC-peptide binding prediction. So the best human substitute alleles for the chicken MHC were chosen from an earlier study (Valdivia-Olarte et al., 2015). Valdivia-Olarte and colleagues compared all the sequences of human MHC-I and MHC-II alleles (available in NetMHCpan and NetMHCIIpan) with the most frequent haplotypes of the chicken MHC alleles and screening only those human MHC alleles which had sequence identities greater than 70%. They used the software MHCcluster (Thomsen et al., 2013) to get heat maps indicating the human MHC-I/II alleles that best substitute its chicken homologues. From this study, three alleles were selected for MHC class I (HLA*B 40:06, HLA*B 41:04 and HLA*B 41:03) and four DRB1 alleles (DRB1:1482, DRB1:1366, DRB1:1310 and DRB1:1445) were chosen for MHC class II.

2.3.2. MHC I binding prediction

For the prediction of MHC-I binding affinity, NetMHCcons 1.1 server was used (http://www.cbs.dtu.dk/services/NetMHCcons). The thresholds for strong binding peptides was set in terms of IC50 value as 2 nM whereas that for weak binders was kept at 50 nM. Therefore, peptides with IC50 $<$ 2 nM were categorized as strong binders and those with 2 nM $<$ IC50 $<$ 50 nM were considered weak binders. For IC50 $>$ 50 nM, lack of binding was considered. The protein sequence was cut into 9 amino acids length of the many possible lengths (Karosiene et al., 2012; Valdivia-Olarte et al., 2015).

2.3.3. MHC II binding prediction

NetMHCIIpan 3.1 server was employed to predict binding of peptides to MHC class II molecules (http://www.cbs.dtu.dk/services/NetMHCcons). The penton base was cleaved into peptides, of 15 amino acids length each, in the server. The server then returned a number of peptides binding to MHC alleles, of which only those peptide (s) were selected which were recognized as strong binders (%Rank $<$ 2) for all the MHC alleles (Andreatta et al., 2015).

2.4. Immunogenic analysis

2.4.1. Cloning of penton base$^{1-225}$ sequence in prokaryotic expression vector

The nucleotide sequence for coding 1–225 amino acids of penton base, corresponding to the predicted linear and discontinues epitope region (penton base$^{1-225}$) was amplified from penton base FL nucleotide sequence (GenBank Acc. No.: HE653773.1) as template using Polymerase Chain Reaction (PCR). Penton base FL gene was available in Structural Biology Lab stock, NIBGE, cloned in pET28a-PreS vector. PreS denotes cleavage site for highly robust PreScission (PreS)/human rhinovirus 3C protease which was introduced into the vector instead of the thrombin protease site, present in PMSJ-Penton vector, used in previous studies (Shah et al., 2012). PCR was performed with forward (GGAATTCCATATGATGTGGGGGTTGCAGCC) and reverse (CGGAATTC TTATTGCACGTTGTTCTGGTGCCC) primers, designed using vector NTI bioinformatics tool. Restriction sites for *Nde* I and *Eco* RI enzymes were inserted into the PCR product at 5′ and 3′ ends respectively during amplification. The amplified PCR product and pET28a-PreS vector were restricted with the restriction enzymes, *Nde* I and *Eco* RI. The purified restriction products were ligated to the vector in fusion with sequence coding for oligohistidine (His_6) tag and a linker “PreS” for purification and tag-removal, if needed, to generate pET28a-PreS-penton base$^{1-225}$ construct. The construct was confirmed by colony PCR and restriction digestion reaction which showed the presence of 675 bp nucleotides sequence, corresponding to the penton base$^{1-225}$ sequence cloned in pET28a-PreS vector.

2.4.2. Protein expression and purification

The constructs, pET28a-PreS-penton base$^{1-225}$ and pET28a-PreS-penton base FL were transformed to *E. coli* BL21-DE3 (Novagen) competent cells using heat shock method (Inoue et al., 1990). Transformed cells were spread on LB-agar plates containing kanamycin (30 μg/mL) and incubated overnight at 37 °C. Morphologically similar, 5–6 colonies were picked from the plates, pre-inoculated in 20 mL LB media (*Kanamycin* 30 μg/mL) and incubated at 37 °C with shaking at 220 rpm. Next morning, the overnight cultures were diluted fifty folds in fresh LB broth supplemented with *kan* (30 μg/mL) in 2-litre flasks and transferred to 37 °C incubator with 220 rpm shaking. The growth phase of the cells was determined after every 45 min using cell density meter (Bio-Wave) until OD_{600} of cultures reached to a value between 0.5 and 0.6. At this stage, cultures were immediately cooled down at 4 °C for 30 min. Protein expression was induced with 1 mM IsoPropyl β-D-ThioGalactoside (IPTG). The expression was continued for 16 h at 18 °C and 220 rpm. Then the *E. coli* cells, producing His_6-PreS-penton base$^{1-225}$ and His_6-PreS-penton base FL proteins, were centrifuged at 4000 rpm for 10 min and the cell pellet was obtained.

To purify proteins, the cell pellet was re-suspended in pre-chilled lysis buffer (50 mM Tris − HCl pH: 7.9, 500 mM NaCl, 5 mM imidazole and 4 mM β-Mercaptoethanol) and passed through cell disrupter (Constant System Ltd.) at 25 kpsi pressure. The cell lysate was centrifuged at 13,000 rpm for 25 min to separate inclusion bodies/cell debris and soluble fraction. The supernatant was transferred to fresh tubes and to purify protein from inclusion bodies, the pellet was re-suspended in equal volume of lysis buffer containing 8 M urea. The re-suspended solution was mixed with needle and left on stirrer for one hour for thorough mixing. A small fraction of supernatant and re-suspended inclusion bodies were analysed on SDS-Polyacrylamide gel.

To avoid protein degradation by intrinsic proteases, the protein solutions were added with 1 mM phenylmethylsulfonyl fluoride (PMSF). The pellet was settled by spinning at 13,000 rpm for 25 min in Beckman Centrifuge.

The supernatant and the re-suspended inclusion bodies were loaded on separate Nickel-nitrilotriacetate (Ni-NTA) agarose columns pre-equilibrated with lysis buffer. To remove non-specific, loosely bound proteins, the column was washed with 25–30 column volume lysis buffer containing 25 mM imidazole. Finally, the purified protein was recovered with lysis buffer containing 250 mM imidazole. All the purification buffers for the re-suspended inclusion bodies were having 8 M urea. Initial fractions were run on SDS-PAGE and pure protein fractions from soluble purified part were pooled, dialyzed against 1x Phosphate Buffer Saline (PBS) pH: 7.4, quantified using Nanodrop spectrophotometer (Thermo Scientific) and stored at 4 °C.

2.4.3. Refolding of denatured proteins

To remove the strong denaturation agent urea and to refold the protein, the purified protein solution was dialyzed against dialysis buffer in subsequent steps. Step-wise dialysis was performed in lysis buffers containing 6 M, 4 M, 2 M and 0 M urea subsequently with the interval of 8 h for each dialysis step and finally the protein was dialyzed against PBS, quantified using Nanodrop spectrophotometer (Thermo Scientific) and analyzed on SDS-PAGE.

2.4.4. Experimental chickens

One-day-old 16 broiler chicks were purchased from commercial

hatchery (Anchor poultry breeders, Faisalabad). It was ensured that the chicks were not pre-vaccinated against FAdV-4 or any other virus and were reared under standard management conditions in an animal house. The experiment was conducted under the regulations of the Institutional Animal Care and Use Committee (IACUC) of Animal Sciences Division, Nuclear Institute for Agriculture and Biology (NIAB), Faisalabad, Pakistan. Chicks were randomly divided into four groups (A, B, C, D) at 7 days of age, having 4 broiler chicks in each group. For all the chicks, same conditions of feed, water, air and hygiene were maintained.

2.4.5. Immunization and challenge studies

Candidate vaccine formulations, having 100 µg total quantity of His_6-PreS-penton base$^{1-225}$ protein or His_6-PreS-penton base FL protein were prepared by stringently mixing 0.47 µg/µL of each protein with Montanide ISA71 V G adjuvant in 70: 30 (w/v) adjuvant: protein ratio (Klimka et al., 2015), for enhanced immunogenicity (Shah et al., 2012). On day 7, a total 500 µL of the above mixture was then injected subcutaneously (s.c.) into the corresponding groups of chicks; group A (100 µg His_6-PreS-penton base$^{1-225}$ + adjuvant) and group B (100 µg His_6-PreS-penton base FL + adjuvant).

On the same day (day 7), each bird in Group C was vaccinated through subcutaneous route by injecting 300 µL of formalin-inactivated commercial vaccine (NIAB Angara), prepared from infected liver homogenate. Group D was kept as challenge control and received only s.c. dose of 500 µL PBS. On day 21, a booster dose of 500 µL of His_6-PreS-penton base$^{1-225}$ and His_6-penton base FL purified recombinant proteins (100 µg + adjuvant) in 3:7 (v/v) ratio of protein: adjuvant, 300 µL commercial vaccine and 500 µL PBS were injected S.C. to their corresponding groups (group A, B, C and D respectively). Blood antisera was collected from birds in each group (from wing veins) before immunization as well as after immunization until 28th day with time interval of 7 days. At the age of 28 days, chickens were challenged with 500 µL of pathogenic FAdV-4-isolated in fresh field cases provided by Animal Sciences Division, Nuclear Institute for Agriculture and Biology (NIAB), Faisalabad, Pakistan, having biological titer $10^{5.5}$ units of lethal dose 50 (LD50) per mL (Shah et al., 2016).

Birds were kept under observation for 7 days post-infection. Mortality was recorded in birds during this period and post-mortem was performed to analyze signs and symptoms related to HPS (Shah et al., 2016).

To determine antibody titer in each group, Indirect Enzyme Linked ImmunoSorbent Assay (ELISA) was performed (Ojkic and Nagy, 2003). His_6-PreS-penton base$^{1-225}$ protein (4 µg) was coated as antigen to determine the antibody titer in group A while His_6-PreS-penton FL protein (4 µg) was coated against antisera produced in group B, C and D in 96 well flat bottom ELISA plates. The serum was added in serial dilutions in PBS to determine the optimal concentration of primary antibody for the assay and finally 1/100 dilution of antisera in PBS was selected for ELISA. Anti-chicken IgG antibodies conjugated with alkaline phosphatase conjugate (A9171- Sigma) were used as secondary antibodies in 1:12,500 dilution. p-nitrophenyl phosphate (MP Biomedicals) was added as substrate to detect the level of secondary antibodies bound to primary antibodies. After 30 min of incubation, the reaction was stopped with 3 M NaOH and data was collected with ELISA microplate reader (Shenzhen heales technology, Co, Ltd) using 405 nm wavelength.

3. Results

3.1. Continuous B-cell epitopes

B-cell epitopes were predicted by using different methods and observing several peptide characteristics for antigenicity. The antigenicity prediction method of Kolaskar and Tongaonkar (Kolaskar and Tongaonkar, 1990) and BepiPred (Jespersen et al., 2017) method were used to predict potent B-cell epitopes. Among the predicted epitopes, only those were chosen for further investigation which had higher antigenicity (Kolaskar and Tongaonkar, 1990) based on parameters like surface accessibility (Emini et al., 1985), flexibility (Karplus and Schulz, 1985), hydrophilicity (Parker et al., 1986) and number of beta turns (Chou and Fasman, 1978). Seventeen epitopes, LE1 (Linear Epitope 1) to LE17 (Linear Epitope 17), in the 528-amino acids long penton base protein were eventually selected from the result of all these tools on the basis of consensus method, described in the Materials and methods section. The peptide lengths, amino acid sequences and positions of these epitopes are given in Table 1.

Table 1
Linear epitopes of the penton base of FAdV-4.

Linear Epitope	Start Position	Sequence	End Position	Length
LE1	5	QPPTSIPPPPPPTELTPSTY	24	20
LE2	27	MVNGYPPPAASAQSCPSSDGQSE	49	23
LE3	60	PTGGRNSIKYRDYTPCRNT	78	19
LE4	86	NKASDIDTYNKDANHSNF	103	18
LE5	111	QDLDADTAA	119	9
LE6	121	ESIQLDNR	128	8
LE7	140	RTNCPNV	146	7
LE8	163	RDPPTSTAPPSAVGSGYSVPGAQYK	187	25
LE9	218	EGHQNNVQKSDI	229	12
LE10	252	GTYVYKGYH	260	9
LE11	299	EDLQGGDI	306	8
LE12	313	DSVDVNDADGE	323	11
LE13	348	QVTGKPVT	355	8
LE14	366	VPNSPANQT	374	9
LE15	402	GFKEDNTTN	410	9
LE16	437	RLENSCQS	444	8
LE17	461	APPMNVSSVCDNQPA	475	15

3.2. Penton base homology model

Five energy minimized comparative protein models were generated by Modeller 9.17 using five different templates in the Protein Data Bank, having highest alignment scores with the penton base (Altschul et al., 1990). The sequence identities of the five structural templates having PDB IDs: 2C6S, 1X 9P, 3IYN, 3ZIF, 4AQQ with the penton base sequence were 53%, 53%, 52%, 45% and 44% respectively. To evaluate the quality of each model, the DOPE (Discrete Optimized Protein Energy) score (Shen and Sali, 2006) i.e. the atomic distance-dependent statistical potential of the five homology models was compared. The homology model generated using the template having PDB ID: 4AQQ, with the lowest DOPE score, was selected since large negative DOPE score is indicator of high quality protein model (di Luccio and Koeh, 2012d).The resulting homology model showed a good sequence coverage (93%) with the template protein.

Though the DOPE score of the chosen protein model was lowest; indicating high quality of the model, yet the sequence identity of the penton base with the corresponding template was low i.e. 44%. Due to low sequence identity, it was assumed that significant information could be missing from certain local regions in the structure such as loops. This affects the quality of the protein model and consequently the structure needed refinement. Thus, loop refinement was carried out for the chosen homology model by Modeller 9.17 (Fiser and Sali, 2003) followed by refinement with GalaxyRefine server (Colovos and Yeates, 1993; Heo et al., 2013).

3.3. Homology model refinement and validation

The homology model was refined using two different web based refinement programs (Fiser and Sali, 2003; Heo et al., 2013). The 3-D model had an N-terminal hanging loop from 1 to 80 amino acids. The model was subjected to refine the loop using Modeller 9.17 program

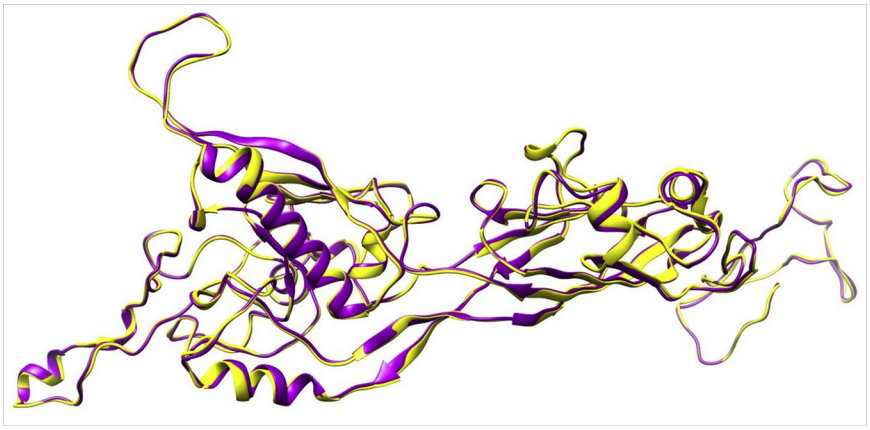

Fig. 1. Refined and un-refined homology model of FAdV-4 penton base.
Homology model no.2 (S1 Table), shown in purple ribbon, is selected from the five proposed refined homology models from the GalaxyRefine web server (Heo et al., 2013). It is overlapped on the homology model before refinement (yellow ribbon).

(Fiser and Sali, 2003) and out of a set of ten proposed models with refined loops, the best contender with lowest value of molpdf (sum of restraint violations) was selected (Yoshikawa et al., 2010). Further, to minimize the structural differences between target and template sequences, resulting from dissimilarities of side-chains (Xiang, 2006), the model was refined making use of GalaxyRefine server (Heo et al., 2013) for correct packing of side-chains. A number of metrics of protein structure accuracy were calculated for each of the five models generated by GalaxyRefine server, as shown in S1 Table. It is known that a structure with numerically low value of molprob score (Chen et al., 2010) and a high GDT-HA (Global Distance Test-High Accuracy) (Heo et al., 2013) is close to a physically realistic model (Dalkas et al., 2014; Pellequer et al., 1993; Su et al., 2012). So, Model 2 (S1 Table) was selected as the optimum model as it had the lowest RMSD (Root Mean Square Deviation), highest GDT-HA and smallest molprob score. This model, as viewed in UCSF Chimera molecular visualization program (Pettersen et al., 2004), is shown in Fig. 1 in purple ribbon, overlapped on the homology model before refinement (in yellow). This refined homology model was then validated by a number of structure validation servers like PROCHECK (Laskowski et al., 1993), ProQ (Cristobal et al., 2001), VERIFY3D (Bowie et al., 1991; Lüthy et al., 1992), ProSA-web (Wiederstein and Sippl, 2007) and ERRAT (Colovos and Yeates, 1993) (S2 Table).

PROCHECK server (Laskowski et al., 1993) was used to derive the popular Ramachandran plot, Φ versus Ψ backbone torsion angles, for the penton base model (S1 Fig) (Lovell et al., 2003). The results of PROCHECK showed a higher proportion of Rama favored residues in the model. Out of 528 amino acid residues, there were a total of 444 non-proline, non-glycine residues for which the Ramachandran plot was attained using PROCHECK, as shown in S1 Fig. S2 Table depicts that the percentage of the non-proline and non-glycine residues in the most favored, additional allowed and generously allowed regions of the plot is 91, 7.9 and 0.5 correspondingly, making a sum total of 99.4%. And only a small fraction is located in the disallowed region (0.6%). In the G-factor (Goodness factor) evaluation, the dihedral angles i.e. Φ-Ψ distribution, χ_1-χ_2 distribution, χ_1 only, χ_3 and χ_4 and ω, altogether yield an average score of 0.26. And the covalent bond lengths and angles return an average score of -0.34. The overall average G-factor turns out to be 0.03 which signifies that the quality of covalent and overall bond/angle distances was appropriate and the probability of the confirmation of the proposed model was high; G-factor above -0.5 corresponds to a reliable model (Laskowski et al., 1993). The computed Ramachandran plot statistics and the average goodness factor indicate that the stereochemistry of the model is acceptable.

From ProQ server (Cristobal et al., 2001), LG score of 1.74 was achieved for the model (S2 Table). As penton base is a long protein with 528 aa (amino acids) and the score lies in the range of 1.5–3.0, the quality of the model is predicted to be good. The overall verify3D (Bowie et al., 1991; Lüthy et al., 1992) score is 66.1% (S2 Table) which shows that more than 65% amino acids have scored > = 0.2 in the 3D/1D profile (S2 Fig). Hence, it may be deduced that the residues of the model fit to their structural environment quite satisfactorily.

The ProSA-web (Wiederstein and Sippl, 2007) *Z*-score of the model was −7.37 (S2 Table) nearer to the X-ray crystallography models, shown as a dark dot in the scatter plot in S3 Fig. This indicates that the homology model of the penton base has good quality comparable to real experimental quality of X-ray crystallography structures.

To determine the ERRAT (Colovos and Yeates, 1993) quality factor, each residue in the model was evaluated by the percentage confidence limit within which the raw score of the residue occurs in comparison with the score distribution of residues in correct protein structures (S4 Fig). The overall quality factor evaluated by ERRAT for the predicted 3D structure of penton base is greater than 80% (S2 Table), which infers that homology modeled structure of the penton base of FAdV-4 is of a decent quality and the residues are reasonably folded.

The ProTSAV scores for quality assessment of the two structures; template and homology model, are shown in S5 Fig. The four regions show the Root Mean Square Deviations; Red (5–8 Å), Orange (2–5 Å), Yellow (2–5 Å), and Green (0–2 Å). It can be seen that the ProTSAV score for the homology model is at yellow-orange interface whereas that for the template structure is in the orange region. Since the scores are in close proximity, it may be inferred that the built model is good and comparable to the template crystal structure. All these tools validated the homology model and ensured that the model was good enough for discontinuous epitope prediction.

3.4. Discontinuous B-cell epitopes

Discontinuous epitopes were predicted using ElliPro (Ponomarenko et al., 2008) which generated two epitopes, DE1 (Discontinuous Epitope 1) and DE2 (Discontinuous Epitope 2), having score greater than 0.7, as depicted in Table 2. Fig. 2(A) shows the first predicted conformational epitope i.e. DE1 with peptide length of 38 residues. The score/ PI for this epitope is 0.777 which signifies that 77.7% of the amino acids are exposed to the surface. Similarly, Fig. 2(B) shows the second discontinuous epitope DE2 with a peptide length of 131 residues and 76.1% of the total 131 amino acid residues are on the outer surface of the structure. The higher surface exposure recommends these conformational epitopes as promising candidates for vaccine development.

Table 2
Antigenic discontinuous epitopes of the penton base of FAdV-4.

Dis-continuous Epitope	Residues	Number of residues	Score
DE1	_:W161, _:K162, _:R163, _:D164, _:P165, _:P166, _:T167, _:S168, _:T169, _:A170, _:P171, _:P172, _:S173, _:A174, _:V175, _:G176, _:S177, _:G178, _:Y179, _:S180, _:V181, _:P182, _:G183, _:A184, _:Q185, _:Y186, _:K187, _:L216, _:S217, _:E218, _:G219, _:H220, _:Q221, _:N222, _:N223, _:V224, _:Q225, _:G268	38	0.777
DE2	_:M1, _:W2, _:G3, _:L4, _:Q5, _:P6, _:P7, _:T8, _:S9, _:I10, _:P11, _:P12, _:P13, _:P14, _:P15, _:P16, _:T17, _:E18, _:L19, _:T20, _:P21, _:S22, _:T23, _:Y24, _:P25, _:A26, _:M27, _:V28, _:N29, _:G30, _:Y31, _:P32, _:P33, _:P34, _:A35, _:A36, _:S37, _:A38, _:Q39, _:S40, _:C41, _:P42, _:S43, _:S44, _:D45, _:G46, _:Q47, _:S48, _:E49, _:L50, _:Y51, _:M52, _:P53, _:L54, _:Q55, _:R56, _:V57, _:M58, _:A59, _:P60, _:T61, _:G62, _:G63, _:R64, _:N65, _:S66, _:I67, _:K68, _:Y69, _:R70, _:D71, _:Y72, _:T73, _:P74, _:C75, _:R76, _:N77, _:T78, _:T79, _:K80, _:F82, _:K87, _:A88, _:S89, _:D90, _:I91, _:D92, _:T93, _:Y94, _:N95, _:K96, _:D97, _:A98, _:N99, _:R104, _:T105, _:T106, _:V107, _:I108, _:H109, _:N110, _:Q111, _:D112, _:L113, _:D114, _:A115, _:D116, _:T117, _:A118, _:A119, _:T120, _:E121, _:S122, _:I123, _:Q124, _:D126, _:N127, _:R128, _:S129, _:S486, _:P489, _:G490, _:L491, _:Q492, _:R496, _:S523, _:S524, _:A525, _:T526, _:L527, _:Q528	131	0.761

Discontinous epitopes were predicted by ElliPro web tool.(Ponomarenko et al., 2008).

3.5. T-cell epitopes

3.5.1. MHC-I epitope

Two peptide stretches of the FAdV-4 penton base sequence i.e. GQSELYMPL$^{45-53}$ and IELDNAAPL$^{324-332}$ were identified to bind strongly with MHC-I alleles (percentage rank ≤ 0.5). Since the peptide GQSELYMPL$^{45-53}$ was predicted by only one of the three human substitute alleles i.e. HLA-B41:04, it was dropped. And the 9-mer peptide sequence IELDNAAPL$^{324-332}$ was selected to be the prospective MHCI T-cell epitope.

3.5.2. MHC-II epitope

A number of 15-mer peptide fragments were identified as strong MHC-II binders with the four human substitute MHC-II alleles as depicted in Table 3. It can be seen from Table 3 that all four human substitute alleles identified the peptide stretch at residue position 145 (VSSFFQSNSVRVRMM$^{145–159}$). The optimal peptide binding core (Andreatta et al., 2015) of this peptide was FFQSNSVRV$^{148-156}$. As this epitope was identified by all MHC-II alleles so it was selected as a promiscuous MHCII T-cell epitope.

3.6. Construction and confirmation of recombinant plasmid

Considering the overall results of the linear and discontinuous epitope prediction and validation, it was deduced that the initial 1–225 amino acid sequence in penton base full length sequence, corresponds to a highly favourable target for vaccine development. The nucleotide sequence for the particular linear and discontinuous epitope region was inserted into pET28a-PreS vector (Ullah et al., 2016). The resultant vector was named pET28a-PreS-penton base$^{1–225}$. Colony PCR and restriction digestion of the construct showed a fragment of the required size on the Agarose gel. Overall strategy and vector design is shown in Fig. 3.

3.7. Expression and purification of His_6-PreS-penton base$^{1–225}$ and His_6-PreS-penton base FL protein

E. coli BL21-DE3 cells harboring pET28a-PreS-penton base$^{1–225}$ and pET28a-PreS-penton base FL were expressed to produce His_6-PreS-penton base$^{1–225}$ and His_6-PreS-penton base FL proteins which were then purified using Ni-NTA chromatography. The His_6-PreS-penton base$^{1–225}$ protein was expressed in inclusion bodies and purified under denaturation condition using chaotropic agent urea whereas His_6-PreS-penton base FL protein was purified from soluble fraction. The purified and refolded His_6-PreS-penton base$^{1–225}$ (~27 kDa) and His_6-PreS-penton base FL (~60 kDa) can be seen at corresponding positions according to their molecular weights on SDS-PAGE (Fig. 4). Purification yield of His_6-PreS-penton base$^{1–225}$ was found to be approximately 3-fold (3.2 mg per liter culture volume) higher than His_6-PreS-penton base FL (1.2 mg per liter culture volume). These results show that the amount of both proteins (in terms of mg/liter) was adequate for further immunization experiments in chicken which usually require 25–100 µg protein for injection to one bird (Shah et al., 2012; Shane, 1996; Wang et al., 2018).

3.8. Immunogenicity and challenge protection test

The immunogenicity studies were performed for the peptide stretch corresponding to the linear and discontinuous epitope region, His_6-PreS-penton base$^{1–225}$ in comparison with His_6-PreS-penton base FL protein and commercial vaccine along with negative control (non-vaccinated-PBS injected only) in chickens and mortalities and disease symptoms were recorded for 7 days post-infection as described in the Materials and Methods section. Among the different immunized groups, half of the birds survived after challenge with FAdV-4. The results revealed equal survival rates (50%) of the birds immunized with His_6-PreS-penton base$^{1–225}$ (Penton 1–225) compared to the birds immunized with His_6-PreS-penton base FL protein (penton) and commercial vaccine (vaccinate), as shown in Table 4. Table 4 also shows the

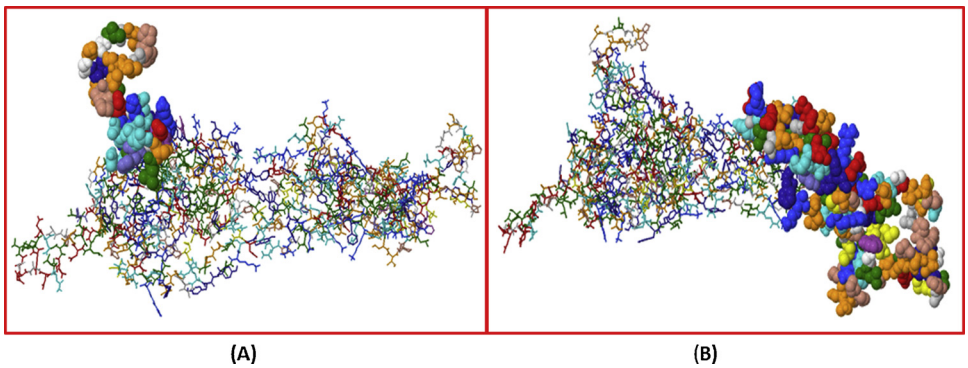

Fig. 2. Discontinuous epitopes for the FAdV-4 penton base predicted by ElliPro web tool (Ponomarenko et al., 2008).
(A) 38 immunogenic residues with 77.7% of the residues exposed to the environment. (B) 131 amino acid residues with a protrusion index of 76.1%. The immunogenic epitopes are depicted as globules on the ball and stick representation of the protein structure.

Table 3
List of the strong MHC-II binders for FAdV-4 penton base.

Allele	Residue Position	Peptide	Core	1-log50k (Chiocca et al., 1996)[a]	Binding Affinity in nanoMolar IC50	% Rank[b]
	145	VSSFFQSNSVRVRMM	FFQSNSVRV	0.785	10.23	0.08
	423	NKIYYQAASTYVQRL	YYQAASTYV	0.741	16.46	0.5
DRB1_1310	422	YNKIYYQAASTYVQR	IYYQAASTY	0.739	16.83	0.5
	454	NEILKQAPPMNVSSV	LKQAPPMNV	0.717	21.39	1
	320	DGEVIELDNAAPLLH	IELDNAAPL	0.699	25.84	1.7
	145	VSSFFQSNSVRVRMM	FFQSNSVRV	0.784	10.40	0.4
DRB1_1366	423	NKIYYQAASTYVQRL	YYQAASTYV	0.739	16.82	1.6
	422	YNKIYYQAASTYVQR	IYYQAASTY	0.739	16.81	1.6
DRB1_1445	145	VSSFFQSNSVRVRMM	FFQSNSVRV	0.472	303.37	1.6
	454	NEILKQAPPMNVSSV	LKQAPPMNV	0.471	307.44	1.7
DRB1_1482	145	VSSFFQSNSVRVRMM	FFQSNSVRV	0.562	114.77	1.6

The MHC-II binders were predicted by NetMHCII Pan 3.1 server with thresholds: Threshold for Strong binding peptides (%Rank): 2%.
Threshold for Weak binding peptides (%Rank): 10%.
[a] Predicted binding affinity (nano Molar IC50) in log scale from 0 to 1.
[b] Percentage Rank of predicted affinity compared to a set of 200,000 random natural peptides. This measure is not affected by inherent bias of certain molecules towards higher or lower mean predicted affinities (Andreatta et al., 2015).

overall strategy for chicken experiments, including details of amount of each injected protein plus adjuvant, treatment/injection days, challenge day and mortalities in birds. In contrast, highest mortality rate was observed in non-immunized birds after challenge with the virus and no bird survived the challenge (100% mortality). All the mortalities occurred between 3–5 days post-infection. Typical signs and symptoms of IBH-HPS were observed in post-mortem results of dead chickens showing straw-colored fluid in pericardial sac and necrotic liver. ELISA results showed a significant increase in titer of antibodies detected in antisera, produced in different groups of birds injected with the recombinant proteins (group A and B) and commercial vaccine (C) as compared to the birds in unimmunized group (D) (Fig. 5).

4. Discussion

In this study, computational screening of the epitopes of a previously identified immunogenic protein by our group (Shah et al., 2012) i.e. penton base of FAdV-4, was conducted along with immunization studies of the predicted epitopes for the development of a peptide-based vaccine against a much neglected broiler disease (HPS) in Pakistan. This in silico approach towards vaccine design is rapid and cost effective (Pushpakumara et al., 2016) and currently in practice for a variety of diseases like Hantavirus Cardiopulmonary Syndrome (Kalaiselvan et al., 2017), Acne vulgaris (Ahmadi et al., 2016), Dengue (Amat-ur-Rasool et al., 2015; Pushpakumara et al., 2016), Hepatitis C (Abdel-Hady et al., 2014) etc (Valdivia-Olarte et al., 2015). An effective vaccine candidate should elicit humoral as well as cell-mediated immune response (Ahmadi et al., 2016), therefore, both B- and T-cell epitope mapping was done to predict peptide epitopes for FAdV-4 penton base FL protein.

Since no single parameter could predict the potential antigenic sites, multiple methods based on different biophysical characteristics of amino acid residues and highly predictive of linear B-cell epitopes were used. The same tools have been employed previously for linear B-cell epitope prediction and were found superior for vaccine design against Saint Louis Encephalitis Virus (Hasan et al., 2013).

The sequences predicted as linear B-cell epitopes (Table 1) are based on diverse peptide characteristics of the penton base. The surface accessibility of the penton base was evaluated to identify whether the amino acid residues are buried or exposed to the solvent. Generally, the amino acid residues located on protein surface serve as antigen binding sites (Gowder et al., 2014). The heptapeptide KYRDYTP$^{68-74}$ of linear epitope LE3, with surface residue 71, has the highest surface accessibility of all i.e. 6.222 (S6 Fig). For antibody recognition, it is very much likely that the antigenic sites are accessible. And since these sites are on surface these are most probably hydrophilic (Parker et al., 1986). The epitopes LE2 and LE15 were found to contain the highest hydrophilicity peptides PSSDGQS$^{42-48}$ and KEDNTTN$^{404-410}$ respectively with corresponding scores of 6.19 and 6.84 at amino acid positions 45 and 407 (S7 Fig).

Besides surface accessibility and hydrophilicity, surface flexibility is also an indicative of the antigenic determinants (Karplus and Schulz, 1985). Karplus and Schulz' method makes use of temperature factors of Cα-atoms i.e. B-factors as a measure for flexibility (Karplus and Schulz, 1985). The predicted linear epitope LE2 also had the highest surface flexibility i.e. 1.128 for the amino acid residue 46 with the peptide stretch running from 43 to 49 (S8 Fig).

It has been reported previously that the epitopes have significantly less secondary structures (strands and helices) and more loops as compared with the remaining antigen (Kringelum et al., 2013). This over-representation of loops is small but important and is in agreement with the perception that antigen-antibody binding sites are flexible regions (Neuvirth et al., 2004). Chou's beta turns was, hence, used as yet another propensity scale for linear B-cell epitope prediction (Su et al., 2012). It exhibits the properties of surface accessibility, hydrophilicity and flexibility which are all correlated with antigenicity (Pellequer et al., 1993). The peptide sequence 11–17 in LE1 was evaluated to have the largest score for beta turns method i.e. 1.44 for amino acid residue 14 followed by 1.43 in LE2 for amino acid position 43 (SCPSSDG$^{40-46}$), as depicted in S9 Fig.

For the Kolaskar and Tongaonkar method (Kolaskar and Tongaonkar, 1990), the LE13-residue 354 (GKPVTVY$^{351-357}$)

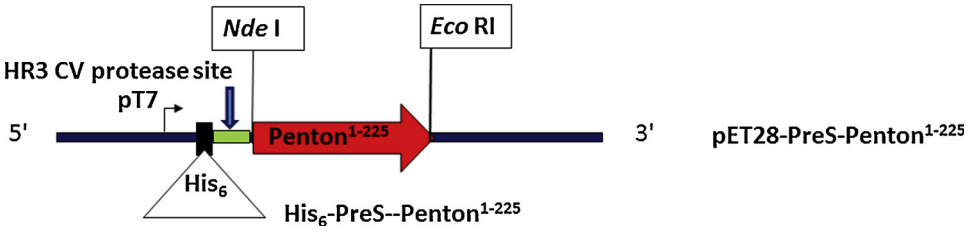

Fig. 3. Cloning strategy for the generation of pET28a-PreS-Penton base$^{1-225}$ plasmid under bacterial T7 promoter in reading frame with six Histidine and HRV 3C protease site, PreS.

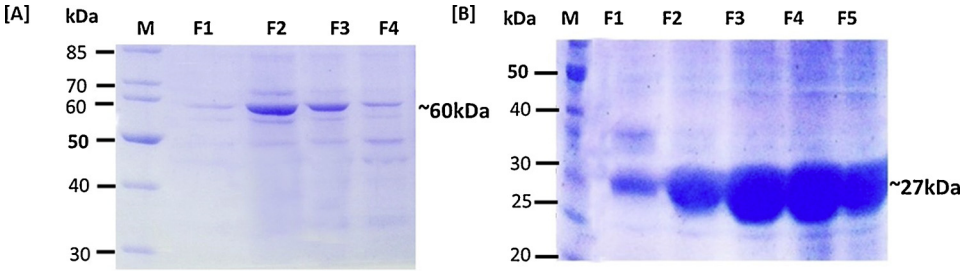

Fig. 4. Purification of His_6-PreS-penton base FL and His_6-PreS-penton base$^{1-225}$ produced in *E. coli* BL21 (DE3) using pET28a-PreS expression vector. [A] His_6-PreS-penton base FL protein expressed in *E. coli* strain BL21 (DE3) and [B] His_6-PreS-penton base$^{1-225}$. Protein expression was carried out using 1 mM IPTG as inducer and post induction temperature of 18 °C for 16 h. Ni-NTA affinity chromatography was used for protein purification. Lanes F1-F5 shows the pure protein obtained after elution from the Ni-NTA columns. The mobility of marker proteins of known molecular mass are shown on the left.

corresponded to the highest score i.e. 1.101 closely chased by residue 252 (VTPGTYV$^{249-255}$) of LE 10 with the value 1.098 (S10 Fig). Furthermore, a random forest algorithm method trained on epitopes annotated from antibody-antigen protein structures was also used for predicting linear B-cell epitopes for the penton base (Jespersen et al., 2017). The maximum score of 3.234 was observed for hepta-peptide SIPPPPP$^{9-15}$ in LE1 (S11 Fig). The average scores for all the linear B-cell epitopes can be seen in S3 Table for further detail.

The web tool ElliPro (Ponomarenko et al., 2008), for the non-linear epitope prediction in the penton base protein, demonstrates a correlation between antigenicity, solvent accessibility and flexibility (Ponomarenko et al., 2008). This tool has been utilized with success in numerous studies for vaccine design/development, for instance Amat-ur-Rasool et al (Amat-ur-Rasool et al., 2015) used it for identifying potent vaccine candidates against dengue virus, and Ren *J*. et al (Ren et al., 2015) utilized it for structure based B-cell epitope prediction for Hand-Foot and Mouth Disease.

In previous studies, it was commonly noticed that most of the continuous epitopes are actually part of a larger discontinuous epitope (Van Regenmortel, 2001). In our case as well, it is evident that most of the B-cell continuous epitopes are parts of the two identified discontinuous epitopes (DE1 and DE2) of lengths 38 and 131 amino acids respectively (Tables 1 and 2). LE1-LE6 form part of DE2 while LE8 and LE9 overlap DE1. This observation enhances the confidence in the accuracy of the predicted B-cell epitopes.

Moreover, it is known that the linear as well as conformational epitopes interact with the antibodies primarily through the loop regions comprising of turns, bends and irregular structures (Dalkas et al., 2014). For antibody recognition of the pathogen protein, the secondary structure of the epitope needs to be intact. This is possible only if the epitope, once isolated, does not get influenced by the environmental conditions and resembles its native conformation- as in the host, during cloning (Strugnell et al., 2011). The intrinsically disordered nature of the loop regions within the protein structure precludes this issue of preservation of native conformation during in vitro protein synthesis and its downstream applications. Thus, preference is given to those peptides which lie in long loops connecting the secondary structure motifs (Reche, 2019). From the predicted secondary structure of penton base, it may be observed that the linear epitopes LE1, LE2, LE3, LE10, LE11, LE12, LE13 and LE15 have loop structure. Hence, keeping in view the preceding results, the peptide stretch 1–225 is identified as the most promising region to evoke the immune response as B-cell epitopes.

The antibody memory response gets vanished easily by the antigen, but T-cell specific epitopes, induce a long-term immune response and dodge antigenic drift (Hasan et al., 2013). The T-cell specific epitopes are, therefore, considered superior and highly favorable for vaccine design and development. In the cell-mediated immunity, CD4+ and CD8+ T-cells have an essential role in evading virus infected cells. Theses T-cells also support in the form of clonal proliferation of B cell against the antigen (Dar et al., 2016).

The major step in triggering this cell-meditated immune response is the recognition of specific peptides bound to MHC class I and II molecules by T-cells. The genomic region which encodes the MHC molecules is exceedingly polymorphic and is composed of thousands of alleles, each encrypting a distinct MHC molecule with unique binding affinity motif. As of June 2016, the Immuno Polymorphism Database (IPD) and International ImMunoGeneTics information system (IMGT)/ Human Leukocyte Antigen (Motamedi et al., 2014) database (Motamedi et al., 2014) reports protein sequences of about 15,000 HLA (Class I and II) alleles. But a very small number of HLA molecules have been characterized with peptide binding data in spite of the huge advancement in high-throughput screening technologies due to enormous technical cost. The situation is poorer for species other than humans (Robinson et al., 2015). Hence, the best human substitute alleles were used instead of chicken alleles for MHC-I and II peptide binding estimation.

The approach used for determining MHC-peptide binding affinities for predicting T-cell epitopes was adopted from a study carried out for vaccine design against Peruvian FAdV-C (Valdivia-Olarte et al., 2015). MHC class I and II molecules present peptides of lengths 8–11 and 12–25 amino acids respectively on the surface of an antigen presenting cell. A 9-mer peptide sequence IELDNAAPL$^{324-332}$ was identified as MHC-I T-cell epitope and a 15-mer peptide stretch VSSFFQSNSVRVRMM$^{145–159}$ was recognized as MHC-II T-cell epitope. The peptide stretch 145–159 coincides with the already predicted 1–225 peptide region for triggering humoral immunity. It was, therefore, concluded that the peptide stretch 1–225 may serve as an excellent candidate for devising a vaccine which can transmit strong humoral and cell-mediated immunity for safeguarding broilers against HPS.

Previously, the immunization and challenge protection tests for the penton base FL protein were performed and higher level of protection

Table 4
Post challenge mortality and percent protection in treatment and control groups.

Group (N = 4)*	Treatment (Total injected)	Treatment/Injection (days)	Age at challenge (days)	Protection
A	Penton 1-225 protein (100 μg/214 μL) + Montanide ISA71 V G adjuvant (386 μL)	7th and 21st	28	50%
B	Penton protein (100 μg/214 μL) + Montanide ISA71 V G adjuvant (386 μL)	7th and 21st	28	50%
C	Commercial vaccine (300 μL)	7th and 21st	28	50%
D	PBS (300 μL)	7th and 21st	28	100%

(N = 4)*: The number of total birds in each group. Mortality in birds occurred between 3–5 days post-challenge (after 28th day).

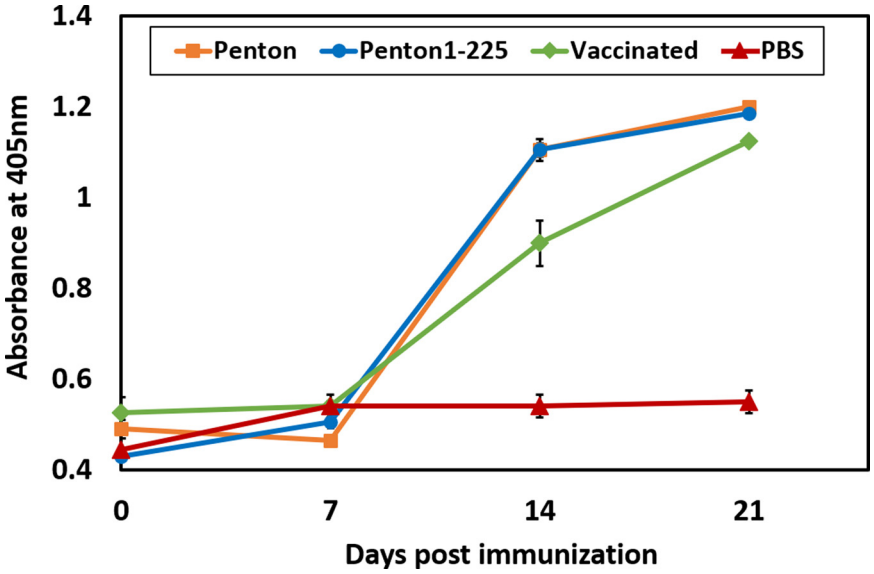

Fig. 5. Antibody titers determined in serum after immunization of different groups of chickens with His_6-PreS-penton base FL (Penton), His_6-PreS-penton base$^{1–225}$ (Penton 1–225), commercial vaccine (vaccinate) and control Phosphate Buffer Saline (PBS) using ELISA. Blood serum samples were collected at different days post-immunization.

against FAdV-4 in chickens was observed. In our study, immunization and protection studies of the predicted epitope region (penton base$^{1–225}$) in comparison with penton base FL were performed in chickens. His_6-PreS-penton base$^{1–225}$ and His_6-PreS-penton base FL protein were produced in *E. coli* using pET28a-PreS expression vector (Shah et al., 2017b) and purified by metal-affinity chromatography. His_6-PreS-penton base$^{1–225}$ can be produced/purified in greater amounts (3-fold higher) than His_6-PreS-penton base FL. The inclusion of His_6-PreS-penton FL protein and commercial vaccine against FAdV-4 (NIAB Angara) in the study were meant for their role as positive control. The results showed equivalent protection ability of penton base$^{1–225}$ as compared to the penton base FL protein and commercial vaccine, containing the whole inactivated virus. The commercial vaccine used in our study offered 50% protection level, comparable to the previously used formalin-inactivated liver organ vaccine, used for the protection of FAdV-4 infections which also conferred 60% (Shah et al., 2012) and 35% protection (Mansoor et al., 2011). The protection level offered by these vaccines was low. Beside low level of protection, an alarming situation is highlighted recently, regarding the use of such vaccines because most of the outbreaks of IBH-HPS occurred post-vaccination and due to this reason, the production of vaccines is minimized in Pakistan and subunit vaccines are suggested (Khan et al., 2005; Mehmood et al., 2011; Shah et al., 2017a). In our study a 50% protection level was observed in all bird groups (injected with adjuvanted penton base FL, penton base$^{1–225}$ and commercial vaccine) as compared to challenge control group, injected with only PBS, where no bird survived, after challenge with pathogenic FAdV-4 having $10^{5.5}$ units LD_{50} titer. Contrary to these results, a higher protection level was observed in past using penton base FL vaccine candidate against FAdV-4 challenge, as compared to commercial vaccines which resulted in 60% protection rate (Shah et al., 2012).

These variations in results may be attributed to some changes in conformation of penton base FL and predicted epitope region (penton base1–225) during purification preparations which resulted in equal protection compared to full length penton base and commercial vaccine. In future, experiment could be performed under multiple conditions to achieve complete assessment of comparative efficacy. At this point, the findings confirm the likely role of the anticipated epitope region, penton base$^{1–225}$, in the immunogenicity and protection against FAdV-4 and control of HPS exactly similar to penton base FL. This outcome further supports the bioinformatics analysis which predicted the initial 1–225 amino acids as a potential antigenic region.

5. Conclusions

A significant amount of resources and time are spent in vaccine development against viruses so this dry lab approach deducing potent B- and T-cell vaccine candidates is a way forward at first stage. In the present study, the N-terminal peptide stretch of 1–225 in penton base full length protein was recognized as a potential epitope for eliciting humoral and cell-mediated immune response. Afterwards, immunogenic analysis was carried out in broiler chicken for verifying the in-silico epitope prediction. It was concluded that penton base$^{1–225}$ could activate equal level of specific immunity against FAdV-4 similar to that of the penton base FL protein in addition to its 3-fold higher purification yield compared to the penton base FL. Such a study for the penton base protein for Pakistani isolate of FAdV-4 has been reported first time. The resulting predicted epitope region in the penton base of FAdV-4 is hereby proposed as a potent vaccine candidate against HPS. This may assist in vaccine design for FAdV-4 infections, making use of penton base$^{1–225}$, in future.

Author contributions

Conceived and designed the experiments: FA, MH, OM, MI, MR. Performed the experiments: FA, ST, MAS, MSS. Analysed the data: FA, ST, MAS, MSS, MH. Wrote the paper: FA, MAS, OM, MI, MR. Read and approved the manuscript: FA, ST, MAS, MSS, MH, OM, MI, MR.

Ethics statement

The study presented in the manuscript does not involve any human subjects. However, this study only involves an experiment on broiler chickens. Institutional Animal Care and Use Committee (IACUC) of Animal Sciences Division, Nuclear Institute for Agriculture and Biology (NIAB), Faisalabad, Pakistan, has approved the study and all applicable international, national and/or institutional guidelines for the care and use of animals were followed.

Declaration of Competing Interest

The authors of this paper declare that they have no conflict of interest.

Acknowledgements

This work was supported by the International Centre for Genetic Engineering and Biotechnology, Italy (Project grant No. CRP/PAK17-01, awarded to Rahman M) and Ph.D. studentships by Higher Education Commission, Pakistan (awarded to Tufail S and Shah MA).

Appendix A. Supplementary data

Supplementary material related to this article can be found, in the online version, at doi:https://doi.org/10.1016/j.virusres.2019.197750.

References

Abdel-Hady, K.M., Gutierrez, A.H., Terry, F., Desrosiers, J., De Groot, A.S., Azzazy, H.M.E., 2014. Identification and retrospective validation of T-cell epitopes in the hepatitis C virus genotype 4 proteome: an accelerated approach toward epitope-driven vaccine development. Hum. Vaccin. Immunother. 10, 2366–2377.
Abdulaziz, T.A., Alattar, M.A., 1991. New syndrome in Iraqi chicks. Vet. Rec. 129, 272.
Ahmadi, A., Farhadi, E., Salimian, J., Amani, J., 2016. Designing a vaccine therapy candidate against Propionibacterium acnes: a bioinformatics approach. Mol. Genet. Microbiol. Virol. 31, 178–186.
Altschul, S.F., Gish, W., Miller, W., Myers, E.W., Lipman, D.J., 1990. Basic local alignment search tool. J. Mol. Biol. 215, 403–410.
Amat-ur-Rasool, H., Saghir, A., Idrees, M., 2015. Computational prediction and analysis of envelop glycoprotein epitopes of DENV-2 and DENV-3 Pakistani isolates: a first step towards Dengue vaccine development. PLoS One 10.
Andreatta, M., Karosiene, E., Rasmussen, M., Stryhn, A., Buus, S., Nielsen, M., 2015. Accurate pan-specific prediction of peptide-MHC class II binding affinity with improved binding core identification. Immunogenetics 67, 641–650.
Asthana, M., Chandra, R., Kumar, R., 2013. Hydropericardium syndrome: current state and future developments. Arch. Virol. 158, 921–931.
Borisov, V.V., Borisov, A.V., Gusev, A.A., 1997. Hydropericardium syndrome in chickens in Russia, xth international congress of the WVPA budapest. Hungary 258.
Bowie, J.U., Luthy, R., Eisenberg, D., 1991. A method to identify protein sequences that fold into a known three-dimensional structure. Science 253, 164–170.
Chen, V.B., Arendall, W.B., Headd, J.J., Keedy, D.A., Immormino, R.M., Kapral, G.J., Murray, L.W., Richardson, J.S., Richardson, D.C., 2010. MolProbity: all-atom structure validation for macromolecular crystallography. Acta Crystallogr. D Biol. Crystallogr. 66, 12–21.
Chiocca, S., Kurzbauer, R., Schaffner, G., Baker, A., Mautner, V., Cotten, M., 1996. The complete DNA sequence and genomic organization of the avian adenovirus CELO. J. Virol. 70, 2939–2949.
Chou, P.Y., Fasman, G.D., 1978. Prediction of the secondary structure of proteins from their amino acid sequence. Adv. Enzymol. Relat. Areas Mol. Biol. 47, 45–148.
Colovos, C., Yeates, T.O., 1993. Verification of protein structures: patterns of nonbonded atomic interactions. Protein Sci. 2, 1511–1519.
Cristobal, S., Zemla, A., Fischer, D., Rychlewski, L., Elofsson, A., 2001. A study of quality measures for protein threading models. BMC Bioinformatics 2.
Dalkas, G.A., Teheux, F., Kwasigroch, J.M., Rooman, M., 2014. Cation–π, amino–π, π–π, and H-bond interactions stabilize antigen–antibody interfaces. Proteins 82, 1734–1746.
Dar, H., Zaheer, T., Rehman, M.T., Ali, A., Javed, A., Khan, G.A., Babar, M.M., Waheed, Y., 2016. Prediction of promiscuous T-cell epitopes in the Zika virus polyprotein: an in silico approach. Asian Pac. J. Trop. Med. 9, 844–850.
di Luccio, E., Koeh, P., 2012d. The H-factor as a novel quality metric for homology modeling. J. Clin. Bioinforma.
Dyson, M.R., Shadbolt, S.P., Vincent, K.J., Perera, R.L., McCafferty, J., 2004. Production of soluble mammalian proteins in Escherichia coli: identification of protein features that correlate with successful expression. BMC Biotechnol. 4, 32.
Emini, E.A., Hughes, J.V., Perlow, D.S., Boger, J., 1985. Induction of hepatitis A virus-neutralizing antibody by a virus-specific synthetic peptide. J. Virol. 55, 836–839.
Erf, G.F., 1997. Immun System Function and Development in Broiler. pp. 109–123.
Fiser, A., Sali, A., 2003. Modeller: generation and refinement of homology-based protein structure models. Meth. Enzymol. 374, 461–491.
Gowder, S.M., Chatterjee, J., Chaudhuri, T., Paul, K., 2014. Prediction and analysis of surface hydrophobic residues in tertiary structure of proteins. The Scientific World Journal.
Hasan, M.A., Hossain, M., Alam, M.J., 2013. A computational assay to design an epitope-based Peptide vaccine against saint louis encephalitis virus. Bioinform. Biol. Insights 7, 347–355.
Heldens, J.G.M., Patel, J.R., Chanter, N., ten Thij, G.J., Gravendijck, M., Schijns, V.E.J.C., Langen, A., Schetters, T.P.M., 2008. Veterinary vaccine development from an industrial perspective. Vet. J. 178, 7–20.
Heo, L., Park, H., Seok, C., 2013. GalaxyRefine: protein structure refinement driven by side-chain repacking. Nucleic Acids Res. 41, W384–388.
Hess, M., 2000. Detection and differentiation of avian adenoviruses A review. Avian Pathol. 29, 195–206.
Inoue, H., Nojima, H., Okayama, H., 1990. High efficiency transformation of Escherichia coli with plasmids. Gene 96, 23–28.
Jantosovic, J., Konard, J., Saly, J., Skardova, I., Kusev, J., Beninghausova, K., 1991. Hydropericardium syndrome in chicks. Veterinastvi 41, 261–263.
Jespersen, M.C., Peters, B., Nielsen, M., Marcatili, P., 2017. BepiPred-2.0: improving sequence-based B-cell epitope prediction using conformational epitopes. Nucleic Acids Res. 45, W24–W29.
Kalaiselvan, S., Sankar, S., Ramamurthy, M., Ghosh, A.R., Nandagopal, B., Sridharan, G., 2017. Prediction of pan-specific B-cell epitopes from nucleocapsid protein of Hantaviruses causing Hantavirus cardiopulmonary syndrome. J. Cell. Biochem. 118, 2320–2324.
Karosiene, E., Lundegaard, C., Lund, O., Nielsen, M., 2012. NetMHCcons: a consensus method for the major histocompatibility complex class I predictions. Immunogenetics 64, 177–186.
Karplus, P.A., Schulz, G.E., 1985. Prediction of chain flexibility in proteins. Naturwissenschaften 72, 212–213.
Khan, A., Sabri, A., Mansoor, M., Hussain, I., 2005. Hydropericardium syndrome in Pakistan: a review. Worlds Poult. Sci. J. 61, 647–654.
Kim, J.N., Byun, S.H., Kim, M.J., Kim, J., Sung, H.W., Mo, I.P., 2008. Outbreaks of hydropericardium syndrome and molecular characterization of Korean fowl adenoviral isolates. Avian Dis. 52, 526–530.
Klimka, A., Michels, L., Glowalla, E., Tosetti, B., Krönke, M., Krut, O., 2015. Montanide ISA 71 VG is advantageous to Freund's adjuvant in immunization against S. Aureus infection of mice. Scand. J. Immunol. 81, 291–297.
Kolaskar, A.S., Tongaonkar, P.C., 1990. A semi-empirical method for prediction of antigenic determinants on protein antigens. FEBS Lett. 276, 172–174.
Kringelum, J.V., Nielsen, M., Padkjær, S.B., Lund, O., 2013. Structural analysis of B-cell epitopes in antibody:protein complexes. Mol. Immunol. 53, 24–34.
Laskowski, R.A., MacArthur, M.W., Moss, D.S., Thornton, J.M., 1993. PROCHECK - a program to check the stereochemical quality of protein structures. J. Appl. Cryst. 26, 283–291.
Lei, H., Peng, X., Jiao, H., Zhao, D., Ouyang, J., 2015. Broadly protective immunity against divergent influenza viruses by oral co-administration of Lactococcus lactis expressing nucleoprotein adjuvanted with cholera toxin B subunit in mice. Microb. Cell Fact. 14, 111.
Lovell, S.C., Davis, I.W., Arendall III, W.B., de Bakker, P.I.W., Word, J.M., Prisant, M.G., Richardson, J.S., Richardson, D.C., 2003. Structure validation by C-alpha geometry: phi,psi and C-alpha deviation. PROTEINS: Struct. Funct. Genet. 50.
Lüthy, R., Bowie, J.U., Eisenberg, D., 1992. Assessment of protein models with three-dimensional profiles. Nature 356, 83–85.
Mansoor, M.K., Hussain, I., Arshad, M., Muhammad, G., 2011. Preparation and evaluation of chicken embryo-adapted fowl adenovirus serotype 4 vaccine in broiler chickens. Trop. Anim. Health Prod. 43, 331–338.
Mansoor, M.K., Hussain, I., Arshad, M., Muhammad, G., Hussain, M.H., Mehmood, M.S., 2009. Molecular characterization of fowl adenovirus serotype 4 (FAV-4) isolate associated with fowl hydropericardium-hepatitis syndrome in Pakistan. Pakistan J. Zool 41, 269–276.
McFerran, J.B., Smyth, J.A., 2000. Avian adenoviruses. Rev. sci. tech. Off. int. Epiz 19, 589–601.
Mehmood, M.D., Muhammad, K., Rabbani, M., Hanif, A., Hussain, I., 2011. In process quality control factors affecting efficacy of Hydropericardium syndrome virus vaccine. Pak. J. Zool. 43.
Motamedi, M.J., Amani, J., Shahsavandi, S., Salmanian, A.H., 2014. In silico design of multimeric HN-F antigen as a highly immunogenic peptide vaccine against newcastle disease virus. Int. J. Pept. Res. Ther. 20, 179–194.
Neuvirth, H., Raz, R., Schreiber, G., 2004. ProMate: a structure based prediction program to identify the location of protein–protein binding sites. J. Mol. Biol. 338, 181–199.
Ojkic, D., Nagy, É., 2003. Antibody response and virus tissue distribution in chickens inoculated with wild-type and recombinant fowl adenoviruses. Vaccine 22, 42–48.
Parker, J.M.R., Guo, D., Hodges, R.S., 1986. New hydrophilicity scale derived from high-performance liquid chromatography peptide retention data: correlation of predicted surface residues with antigenicity and X-ray-derived accessible sites. Biochemistry 25, 5425–5432.
Pellequer, J.-L., Westhof, E., Van Regenmortel, M.H.V., 1993. Correlation between the location of antigenic sites and the prediction of turns in proteins. Immunol. Lett. 36, 83–100.
Pettersen, E.F., Goddard, T.D., Huang, C.C., Couch, G.S., Greenblatt, D.M., Meng, E.C., Ferrin, T.E., 2004. UCSF Chimera–a visualization system for exploratory research and analysis. J. Comput. Chem. 25, 1605–1612.
Pitcovskia, J., Gutterb, B., Gallilib, G., Goldwaya, M., Perelmanb, B., Grossa, G., Krispela, S., Barbakovb, M., Michaelb, A., 2003. Development and large-scale use of recombinant VP2 vaccine for the prevention of infectious bursal disease of chickens. Vaccine 21, 4736–4743.
Ponomarenko, J., Bui, H.H., Li, W., Fusseder, N., Bourne, P.E., Sette, A., Peters, B., 2008. ElliPro: a new structure-based tool for the prediction of antibody epitopes. BMC Bioinformatics 9, 514.
Pushpakumara, P., Premarathne, P., Goonasekara, C., 2016. Characterisation of B cell epitopes of dengue virus NS1 protein using bioinformatics approach. J. Sci. Found. 44, 417–425.
Reche, P. Predicting Antigenic Peptides. 10/04/2018. http://imed.med.ucm.es/Tools/antigenic.html.
Ren, J., Wang, X., Zhu, L., Hu, Z., Gao, Q., Yang, P., Li, X., Wang, J., Shen, X., Fry, E.E., Rao, Z., Stuart, D.I., 2015. Structures of coxsackievirus A16 capsids with native antigenicity: implications for particle expansion, receptor binding, and immunogenicity. J. Virol. 89, 10500–10511.
Robinson, J., Halliwell, J.A., Hayhurst, J.D., Flicek, P., Parham, P., Marsh, S.G., 2015. The IPD and IMGT/HLA database: allele variant databases. Nucleic Acids Res. 43, D423–431.
Shafique, M., Khan, M.Z., Javeed, M.T., Khan, A., 1993. Lesions of hydropericardium

syndrome in embryonating eggs and in broiler chicks under immunosuppression. Singap Vet J 16, 58–64.
Shah, M., Ashraf, A., Khan, M., Rahman, M., Habib, M., Chughtai, M., Qureshi, J., 2017a. Fowl adenovirus: history, emergence, biology and development of a vaccine against hydropericardium syndrome. Arch. Virol. 162, 1833–1843.
Shah, M.A., Ullah, R., De March, M., Shah, M.S., Ismat, F., Habib, M., Iqbal, M., Onesti, S., Rahman, M., 2017b. Overexpression and characterization of the 100K protein of Fowl adenovirus-4 as an antiviral target. Virus Res. 238, 218–225.
Shah, M.S., Ashraf, A., Khan, M.I., Rahman, M., Habib, M., Qureshi, J.A., 2016. Molecular cloning, expression and characterization of 100K gene of fowl adenovirus-4 for prevention and control of hydropericardium syndrome. Biologicals: journal of the International Association of Biological Standardization 44, 19–23.
Shah, M.S., Ashraf, A., Rahman, M., Khan, M.I., Qureshi, J.A., 2012. A subunit vaccine against hydropericardium syndrome using adenovirus penton capsid protein. Vaccine 30, 7153–7156.
Shane, S.M., 1996. Hydropericardium-hepatitis syndrome, the current world situation. Zootec Int 18, 20–27.
Shen, M., Sali, A., 2006. Statistical potential for assessment and prediction of protein structures. Protein Sci. 15, 2507–2524.
Singh, A., Kaushik, R., Mishra, A., Shanker, A., Jayaram, B., 2016. ProTSAV: a protein tertiary structure analysis and validation server. BBA - Proteins and Proteomics 1864, 11–19.
Smith, J.G., Silvestry, M., Lindert, S., Lu, W.Y., Nemerow, G.R., Stewart, P.L., 2010. Insight into the mechanisms of adenovirus capsid disassembly from studies of defensin neutralization. PLoS Pathog. 6.
Strugnell, R., Zepp, F., Cunningham, A., Tantawichien, T., 2011. Vaccine antigens. Perspect. Vaccinol. 1, 61–88.
Su, C.-H., Pal, N.R., Lin, K.-L., Chung, I.-F., 2012. Identification of amino acid propensities that are strong determinants of linear B-cell epitope using neural networks. PLoS One 7, 10.
Thomsen, M., Lundegaard, C., Buus, S., Lund, O., Nielsen, M., 2013. MHCcluster, a method for functional clustering of MHC molecules. Immunogenetics 65, 655–665.
Ullah, R., Shah, M.A., Tufail, S., Ismat, F., Imran, M., Iqbal, M., Mirza, O., Rhaman, M., 2016. Activity of the human rhinovirus 3C protease studied in various buffers, additives and detergents solutions for recombinant protein production. PLoS One 11, e0153436.
Valdivia-Olarte, H., Requena, D., Ramirez, M., Saravia, L.E., Izquierdo, R., Falconi-Agapito, F., Zavaleta, M., Best, I., Fernández-Díaz, M., Zimic, M., 2015. Design of a predicted MHC restricted short peptide immunodiagnostic and vaccine candidate for Fowl adenovirus C in chicken infection. Bioinformation 11, 460–465.
Van Regenmortel, M.H.V., 2001. Antigenicity and immunogenicity of synthetic peptides. Biologicals 29, 209–213.
Voss, M., Vielitz, E., Hess, M., Prusas, C.H., Mazaheri, A., 1996. Aetiological aspects of hepatitis and HPS caused by pathogenic adenoviruses in different countries. In: Rauischholz-hausen (Ed.), International Symposium on Adenovirus and Reovirus Infection in Poultry, pp. 75–78.
Wang, X., Tang, Q., Chu, Z., Wang, P., Luo, C., Zhang, Y., Fang, X., Qiu, L., Dang, R., Yang, Z., 2018. Immune protection efficacy of FAdV-4 surface proteins fiber-1, fiber-2, hexon and penton base. Virus Res. 245, 1–6.
Webb, B., Sali, A., 2014. Protein structure modeling with MODELLER. In: Kihara, D. (Ed.), Protein Structure Prediction. Springer New York, New York, NY, pp. 1–15.
Wiederstein, M., Sippl, M.J., 2007. ProSA-web: interactive web service for the recognition of errors in three-dimensional structures of proteins. Nucleic Acids Res. W407–W410.
Xiang, Z., 2006. Advances in homology protein structure modeling. Curr. Protein Pept. Sci. 7, 217–227.
Yang, H., Chen, H., Jin, M., Xie, H., He, S., Wei, J.F., 2016. Molecular cloning, expression, IgE binding activities and in silico epitope prediction of per a 9 allergens of the American cockroach. Int. J. Mol. Med. 38, 1795–1805.
Yang, X., Yu, X., 2009. An introduction to epitope prediction methods and software. Rev. Med. Virol. 19, 77–96.
Yoshikawa, E., Miyagi, S., Dedachi, K., Ishihara-Sugano, M., Itoh, S., Kurita, N., 2010. Specific interactions between aryl hydrocarbon receptor and dioxin congeners: ab initio fragment molecular orbital calculations. J. Mol. Graph. Model. 29, 197–205.